Special Issue Article

A Forgotten Chiral Spiro Compound Revisited: 3,3'-Dimethyl-3*H*,3'*H*-2,2'-spirobi[[1,3]benzothiazole]

ANGÉLIQUE LINDAMULAGE DE SILVA,[1] VESNA RISSO,[1] MARION JEAN,[1] MICHEL GIORGI,[2] VALÉRIE MONNIER,[2] JEAN-VALÈRE NAUBRON,[2] NICOLAS VANTHUYNE,[1] DANIEL FARRAN,[1] AND CHRISTIAN ROUSSEL[1]*

[1]*Aix Marseille Université, Centrale Marseille, CNRS, iSm2 UMR 7313, 13397, Marseille, France*
[2]*Spectropôle, Aix Marseille Université, Marseille, France*

ABSTRACT The title compound was obtained as a side product during dimerization-oxidation steps of the carbene generated from *N*-methylbenzothiazolium iodide. Chromatography on (*S*,*S*)-Whelk O1 column showed on cooling a typical plateau shape chromatogram indicating an exchange between two enantiomers on the column. The thermal barrier to racemization was determined (85 kJ.mol^{-1} at 10 °C) by dynamic high-performance liquid chromatography (DHPLC).The absolute configuration of the first (*M*) and second eluted (*P*) enantiomers on the (*S*, *S*)-Whelk O1 column was established by comparing the reconstructed circular dichroism (CD) spectra from the CD detector signal and the calculated CD spectrum of the (*P*) enantiomer. Mass spectrometry revealed that 3,3'-dimethyl-3*H*,3'*H*-2,2'-spirobi[[1,3]benzothiazole] can be viewed as a masked thiophenate attached to a benzothiazolium framework. *Chirality 27:716–721, 2015*. © 2015 Wiley Periodicals, Inc.

KEY WORDS: axial chirality; racemization barrier; spiro heterocycle; carbene dimerization; oxidation of carbene dimer

We targeted the synthesis of the 10-membered ring **1** (Scheme 1) through the dimerization of the carbene generated from N-methylbenzothiazolium iodide in the presence of triethylamine followed by air oxidation according to Murphy and coll. in 1999.[1]

The reaction is reported to be quantitative for the N-ethyl analog but for unclear reasons the outcome of our reaction was different, leading to three compounds we isolated in low yields by column chromatography in addition to **1** (Scheme 2). N-methyl benzothiazolinone **2**, the spiro-compound **3**, which resulted from a partial oxidation of the dimerized carbene, and a nice crystalline spiro compound **4** issuing from the decarbonylation of **3** were identified.

The characterization of these three compounds with modern techniques followed by a literature search led us to the conclusion we were "reinventing" an already described outcome of that reaction long before the extraordinary development of N-heterocyclic carbenes (NHCs) in chemistry.[2,3] The spiro compound **4** was solely reported or mentioned during a period ranging between 1964 and 1978 and was recalled in a review in 2005.[4–12] A possible mechanism for the formation of **3** and **4** has been proposed.[5] As a proof of the memory loss for compounds issued from that reaction, it was particularly frustrating to see that Metzger et al. were the very first to describe compound **4** more than 50 years ago in the laboratory where the present study was conducted in Marseilles, long before the characterization of **1**.[4] During our efforts to identify the spiro compound **4**, some unprecedented features appeared; they are reported herein.

MATERIALS AND METHODS

General Information

Commercially reagent grade chemicals were used as received without additional purification. All reactions were followed by thin-layer chromatography (TLC) (Kieselgel 60 F-254). TLC spots were visualized with UV (254 nm). Column chromatography was performed on silica gel (60–200 mesh). Dichloromethane used for purification by column chromatography contained amylene as stabilizer. Nuclear magnetic resonance (NMR) spectra were recorded on Bruker Avance DRX-400 MHz or Bruker Avance III - 600 MHz instruments. Chemicals shifts in ^{1}H NMR and ^{13}C NMR spectra are reported as parts per million downshift from tetramethylsilane and coupling constants are reported in Hertz. When necessary, resonances were assigned using 2D experiments (COSY, HMBC, HSQC). HRMS (ESI) were recorded on a Waters SYNAPT G2 HDMS mass spectrometer or a QStar Elite (Applied Biosystems, Foster City, CA, SCIEX) equipped with a TOF analyzer. High-resolution mass spectrometry (MS), tandem MS/MS, and traveling wave ion-mobility mass spectrometry (TWIM MS) experiments were performed with a Waters Synapt G2 HDMS quadrupole/time-of-flight (Q/ToF) tandem mass spectrometer (Manchester, UK), using the following parameters: ESI capillary voltage: +2.8 kV; sampling cone voltage: +20 V range;

[This article is part of the Thematic Issue: "Chirality in Separation Science and Molecular Recognition Honoring Prof. F. Gasparrini." See the first articles for this special issue previously published in Volume 27:9. More special articles will be found in this issue as well as in those to come.]

*Correspondence to: Christian Roussel, Aix Marseille Université, Centrale Marseille, CNRS, iSm2 UMR7313,13397, Marseille, France. E-mail: christian.roussel@univ-amu.fr

Received for publication 14 June 2015; Accepted 9 July 2015
DOI: 10.1002/chir.22492
Published online 25 August 2015 in Wiley Online Library (wileyonlinelibrary.com).

© 2015 Wiley Periodicals, Inc.

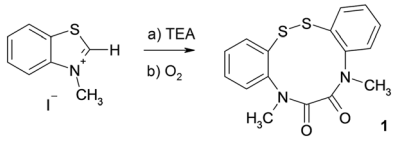

Scheme 1. Preparation of 10-membered ring 1.

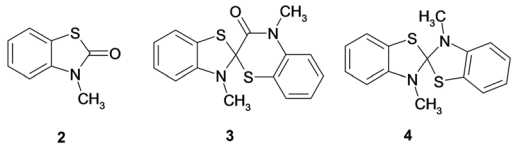

Scheme 2. Side products isolated during the synthesis of 1.

desolvation gas (N_2) flow: 100 L h^{-1} ; transfer CE: 4 eV; trap gas flow: 2 mL min^{-1} (Ar); helium cell gas flow: 180 mL min^{-1}; ion mobility cell gas flow 90 mL min^{-1} (3.45 mbar N_2); source temperature: 20 °C; desolvation temperature: 35 °C; IM traveling-wave height: 40 V; and IM traveling wave velocity: 650 m s^{-1}. Data analyses were conducted using the MassLynx 4.1 program provided by Waters. Chiral high-performance liquid chromatography (HPLC) analyses were achieved on a unit composed of a Merck D-7000 system manager, a Merck-Lachrom L-7100 pump, a Merck-Lachrom L-7200 autosampler, a Merck-Lachrom L-7360 oven, a Merck-Lachrom L-7400 UV-detector, and a Jasco CD-1595 detector. (*S*,*S*)-Whelk O1 column (250*4.6 mm) was purchased from Regis Technologies (Morton Grove, IL).

Synthesis

To a solution of triethylamine (0.58 ml, 4.32 mmol) in acetonitrile (9.30 ml) was added at 0 °C the *N*-methyl-benzothiazolium iodide (0.600 g, 2.16 mmol). The mixture was allowed to warm to room temperature and stirred for 24 h. The solvent was then removed under reduced pressure and dichloromethane (10 ml) was added. The organic layer was washed with water (20 ml), dried on $MgSO_4$, and evaporated under reduced pressure. The crude product was purified by column chromatography (eluent: CH_2Cl_2/MeOH 99.5/0.5) allowing to isolate compounds **1** (15–40%), **2** (5–12%), **3** (5–15%), and **4** (5–15%).

Physical data for 5,8-dimethyldibenzo[*c*,*i*][1,2,5,8]-dithiadiazecine-6,7(5*H*,8*H*)-dione 1. Yellow solid; Rf = 0.45 (CH_2Cl_2/MeOH 99.5/0.5); ^{1}H NMR (400 MHz, $CDCl_3$, δ): 3.04 (s, 6H; CH_3), 7.34-7.41 (m, 2H; Ar H), 7.48-7.51 (m, 4H; Ar H), 7.70-7.75 (m, 2H; Ar H); ^{13}C NMR (100 MHz, $CDCl_3$, δ): 36.7 (CH_3), 130.0 (CH), 132.0 (CH), 132.3 (CH), 136.4 (C), 138.3 (CH), 144.5 (C), 163.8 (C = O); HRMS (ESI, *m/z*): $[M+H]^+$ calcd for $C_{16}H_{15}N_2O_2S_2$, 331.0569; found, 331.0569.

Physical data for 3-methyl-1,3-benzothiazol-2(3*H*)-one 2. Yellow oil; Rf = 0.73 (CH_2Cl_2/MeOH 99.5/0.5); ^{1}H NMR (400 MHz, $CDCl_3$, δ): 3.46 (s, 3H; CH_3), 7.04 (d, *J* = 8.2 Hz, 1H; Ar H), 7.17 (td, *J* = 7.7 Hz, *J* = 1.1 Hz,1H; Ar H), 7.34 (td, *J* = 7.8 Hz, *J* = 1.2 Hz, 1H; Ar H), 7.43 (dd, *J* = 7.8 Hz, *J* = 0.9 Hz,1H; Ar H). ^{1}H NMR data are consistent with a commercial sample and the literature.[13]

Physical data for 3',4-dimethyl-3'*H*-spiro[1,4-benzothiazine-2,2'-[1,3]benzothiazol]-3(4*H*)-one 3. White solid, mp: 136 °C; Rf = 0.82 (CH_2Cl_2/MeOH 99.5/0.5); ^{1}H NMR (400 MHz, $CDCl_3$, δ): 3.15 (s, 3H; CH_3), 3.56 (s, 3H; CH_3), 6.61 (d, *J* = 8.0 Hz, 1H; Ar H), 6.78 (td, *J* = 7.6 Hz, *J* = 1.0 Hz, 1H; Ar H), 6.96 (dd, *J* = 7.6 Hz, *J* = 1.1 Hz,1H; Ar H), 7.08-7.13 (m, 2H; Ar H), 7.17 (dd, *J* = 8.2 Hz, *J* = 0.9 Hz,1H; Ar H), 7.30 (dd, *J* = 7.7 Hz, *J* = 1.4 Hz,1H; Ar H), 7.33-7.38 (m, 1H; Ar H); ^{13}C NMR (150 MHz, $CDCl_3$, δ): 32.7 (CH_3), 34.0 (CH_3), 89.3 (C), 108.3 (CH), 118.2 (CH), 120.3 (CH), 121.4 (C), 122.1 (CH), 122.6 (C), 124.4 (CH), 126.5 (CH), 128.0 (CH), 130.9 (CH), 139.1 (C), 145.9 (C), 162.0 (C = O); HRMS (ESI, *m/z*): $[M+H]^+$ calcd for $C_{16}H_{15}N_2OS_2$, 315.0620; found, 315.0631; $[M+Na]^+$ calcd for $C_{16}H_{14}N_2OS_2Na$, 337.0440; found, 337.0447.

Physical data for 3,3'-dimethyl-3*H*,3'*H*-2,2'-spirobi[[1,3]-benzothiazole 4. White crystals, mp: 233 °C; Rf = 0.91 (CH_2Cl_2/MeOH 99.5/0.5); ^{1}H NMR (400 MHz, $CDCl_3$, δ): 2.87 (s, 6H; CH_3), 6.45-6.49 (m, 2H; Ar H), 6.77 (td, *J* = 7.5 Hz, *J* = 1.0 Hz, 2H; Ar H), 7.03-7.08 (m, 4H; Ar H); ^{13}C NMR (100 MHz, $CDCl_3$, δ): 29.6 (CH_3), 106.9 (CH), 118.7 (C), 119.5 (CH), 120.9 (CH), 123.5 (C), 125.7 (CH), 142.6 (C); HRMS (ESI, *m/z*): $[M+H]^+$ calcd for $C_{16}H_{15}N_2OS_2$, 287.0671; found, 287.0681.

It is worth mentioning that compounds **3** and **4** were kept in the solid state to prevent decomposition.

X-ray analysis of 4. CCDC-1404056 contains the supplementary crystallographic data for this article. These data can be obtained free of charge from the Cambridge Data Centre via www.ccdc.cam.ac.uk/data_request/cif.

Calculations. Based on B3LYP/6-311G(df,p) optimized geometry of the unique conformation of **4**, the ECD and UV spectra were calculated using time-dependent Density Functional Theory (TD-DFT)[14,15] with CAM-B3LYP functional[16] and 6-31++G(d,p) basis set. Calculations were performed for vertical 1A singlet excitation using 30 states. For a comparison between theoretical results and the experimental values, the calculated UV and ECD spectra have been modeled with a Gaussian function, using a half-width of 0.31 eV. Due to the approximations of the theoretical model used, an offset almost constant was observed between measured and calculated frequencies. Using UV spectra, all frequencies were calibrated by a factor of 1.1. All calculations were performed using Gaussian 09 package.[17]

RESULTS AND DISCUSSION

The spiro compound **4** is axially chiral. The first single crystal x-ray structure determination of **4** revealed, as expected, the *M* and *P* forms in the cell (Fig. 1).

Interestingly, the molecule that presents a noncrystallographic two-fold axis centered on the spirocarbon displays unsymmetric behavior at the level of its intermolecular interactions. The calculation of Hirshfeld surfaces[18] reveals that the interactions within the crystal are mainly dominated by CH/π and π/π interactions: the fingerprint of compound **4** is very close to that of polycyclic aromatic compounds (fig. 5 in Supporting Information).[19] However, one sulfur atom is in short contact with a hydrogen of a symmetry-related molecule while the other is in short contact with another sulfur atom in the crystal, the latter being the stronger intermolecular interaction

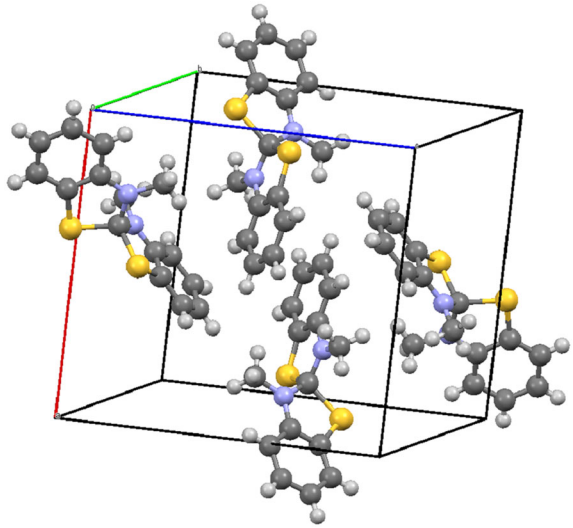

Fig. 1. Single crystal x-ray of **4**.

(figs. 6 and 7 in Supporting Information). That difference in the nature of short contacts is probably at the origin of the difference in length between the two sulfur-central carbon bonds (1.85 and 1.88 Å, respectively). This dissymmetry within the crystal structure of **4** is also illustrated on the N-CH_3 moieties, as the two N-CH_3 bond lengths are significantly different: 1.436 and 1.374 Å, respectively. The methyl group of the longer N-CH_3 bond and its connected aromatic ring are involved in several intermolecular CH-π interactions with symmetry-related molecules (fig. 8 in Supporting Information).

Spiro compound **4** was submitted to a screening on several chiral stationary phases using various mobile phases. At room temperature, a single peak was noticed on most of the coated or immobilized polysaccharide stationary phases, while a broad distorted peak was obtained on the so-called (*S*,*S*)-Whelk O1 eluted with a mixture of heptane/2-PrOH. On cooling, a typical plateau shape chromatogram was obtained, indicating an exchange between two enantiomers on the column (Fig. 2).[20–35]

As usual, the plateau was composed of the racemate and thus gave no signal during chiroptical detection. With the aid of the Trapp and Schurig equation,[36–38] a thermal barrier to racemization of 85 kJ.mol^{-1} at 10 °C was determined, indicating a relatively fast exchange at room temperature and precluding further easy isolation of the enantiomers. Compound **4** presents a unique feature in which a carbon atom bears two nitrogen atoms and two sulfur atoms. The breaking of one carbon-sulfur bond may lead to the rather stabilized intermediate **5** (Scheme 3)

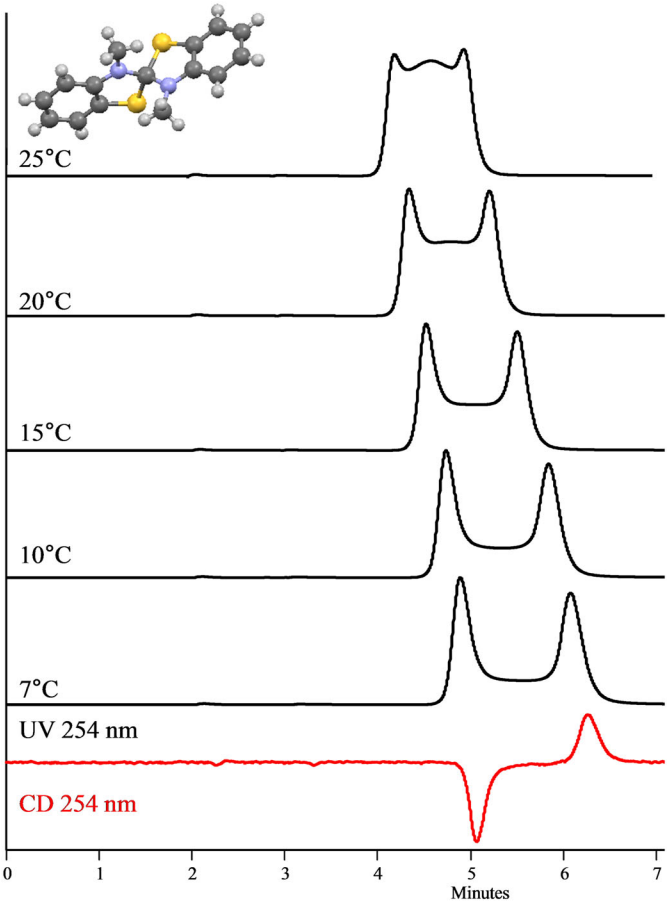

Fig. 2. Chromatogram of **4** on (*S*,*S*)-Whelk-O1 column (90:10 v:v heptane/2-PrOH, 1.5 ml.min^{-1}, UV and CD traces at 254 nm at different temperatures. ΔG = 85 kJ.mol^{-1} at 10 °C).

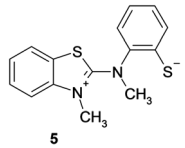

5

Scheme 3. Open form intermediate **5** on the racemization pathway of **4**.

in which a fast rotation around the N-aryl bond and further formation of the C-S bond from both sides of the achiral benzothiazolium salt results in racemization.

The thermal barrier of 85 kJ.mol^{-1} thus reflects the weakness of the C-S bonds, the stabilization of the open form **5**, and includes a statistical contribution since the two C-S bond are equivalently prone to break. According to barrier determination, the C-S bond is particularly weak in spiro compound **4**.

Polarimetric detection with a Jasco OR-1590 detector, which combines the signals between 300 and 900 nm, did not produce any signal for the front and back eluting aisles. On the other hand, the circular dichroism (CD) detector set at 254 nm showed that the enantiomer presenting a negative CD sign at that wavelength and in the mobile phase was the less retained enantiomer on the (*S*,*S*)-Whelk O1 column. The first eluted enantiomer constantly gave a negative CD sign at 254 nm when different mobile phases were applied on the (*S*,*S*)-Whelk O1 column at 15 °C. These mobile phases were composed of heptane/chloroform (90:10 v:v), heptane/ethylacetate (90:10 or 95:5 v:v), heptane/THF (98:2 v:v), or heptane/tertiobutanol (90:10 v:v). It was tempting to determine the order of elution and thus the chiral recognition of the enantiomers by the (*S*,*S*)-Whelk O1 chiral column through a calculation of the CD spectrum for one enantiomer of **4**.

The calculated CD spectra for (*P*)-**4** (Fig. 3a) showed a large positive band centered at ~260 nm and a large negative band centered at ~300 nm after a calibration from the comparison of the calculated and experimental UV spectra signal (fig. 10 in Supporting Information). Since the region where the CD detector was set (254 nm) is quite close to the maximum of the calculated band (260 nm), we were quite confident that the first eluted enantiomer is the (*M*) one.

In order to confirm the assignment, several injections from the same vial, to ensure the same concentration, were performed on the (*S*,*S*)-Whelk O1 at 15 °C in a mobile phase consisting of 90:10 v:v heptane/2-PrOH. The UV detector was set at 254 nm while the CD detector was set at different wavelengths (15 measurements), one for each injection. The UV traces served to track any concentration changes or artifacts, while the CD traces were collected for the first and second eluted enantiomer in exchange (fig. 9 in Supporting Information). It was thus possible to reconstruct the CD spectra of the first and second aisles of the plateau which correspond to the first and second eluted enantiomers (Fig. 3b). Comparison of the reconstructed CD spectra with the calculated one for (*P*)-**4** nicely shows that the (*P*) enantiomer (second eluted) has the higher affinity with the (*S*,*S*)-Whelk-O1 chiral selector. The fitting between calculated and reconstructed CD spectra is not as good for low wavelengths (<240 nm) than for the two major bands at longer wavelengths (>240 nm).

The mass spectrometry results deserve some comments since they were quite puzzling when we were trying to elucidate the structure of **4**. The mass spectra after electrospray ionization in positive mode (Fig. 4a) showed the presence of

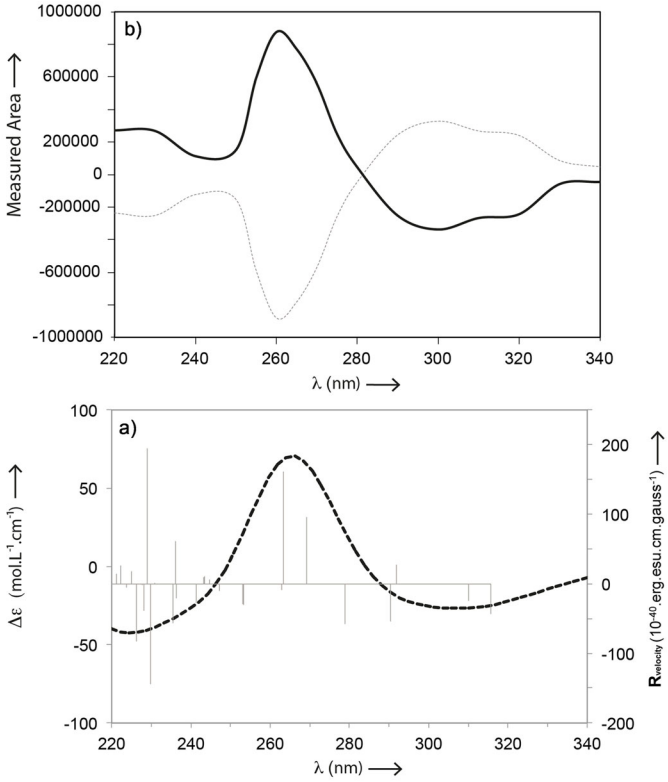

Fig. 3. Calculated CD for the (*P*)-**4** enantiomer in vacuum (a) and reconstructed experimental CD for the first (dotted line) and second eluted enantiomers (plain line) from data generated on (*S*,*S*)-Whelk O1 in a mobile phase composed of heptane/2-PrOH (90:10) at 15 °C (b).

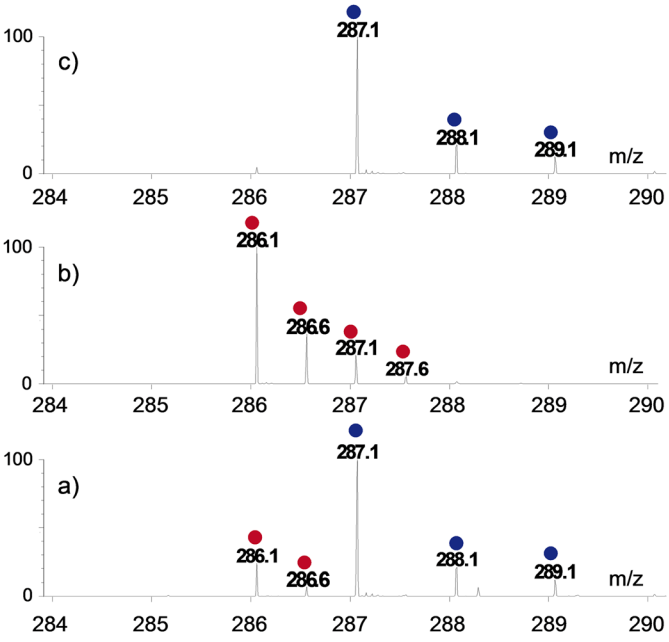

Fig. 4. (a) Mass spectra of **4** in positive electrospray mode; (b) doubly charged m/z 286 ion; and (c) singly charged m/z 287 ion extraction after ionic mobility separation.

a doubly charge ion corresponding to m/z 286 (red spots) in close vicinity of a singly charged ion m/z 287 (blue spots).

These differently charged ions were cleanly separated thanks to ionic mobility (Fig. 4b,c). Exact mass measurements on m/z 287 ion showed that it corresponded to the ion $C_{15}H_{15}N_2S_2^+$ [exp. : m/z 287.0665, th : m/z 287.0671, delta : −2.1 ppm] associated with [4 + H^+]. Exact mass measurement on m/z 286 ion showed that it corresponded to the doubly charged ion $C_{30}H_{28}N_4S_4^{2+}$ [exp. : m/z 286.0595, th : 286.0593, delta : +0.7 ppm]. This latter compound fitted with a dimerization of **5** through a disulfide bond.

The occurrence of that dimer during a very soft electrospray ionization (or during the sample preparation) is in the line of the low barrier to racemization occurring through **5** which gained the status of intermediate after the MS results. In the presence of methanol, the status of low populated intermediate for **5** might be validated by the observation of an ion m/z 317 corresponding to $C_{16}H_{17}N_2OS_2^+$ [exp. : m/z 317.0781, th : m/z 317.0777, delta: +1.3 ppm] which results from the addition of MeO^- to **5**. In the same way, in the presence of I^-, an m/z 413 ion is observed, corresponding to $C_{15}H_{14}N_2S_2I^+$ [exp.: m/z 412.9641, th : m/z 412.9638, delta: +0.7 ppm] which results from the addition of I^- to **5**.

In the literature, several spiro compounds with two oxygen and two unsaturated carbon atoms linked to the central carbon atom (such as in spiropyrans) have been intensively studied for their valuable thermochromic or(and) photochromic properties (Scheme 4). The open forms are particularly stabilized. Okamoto et al. resolved the enantiomers of compounds **6** by liquid chromatography on a chiral poly(triphenylmethyl methacrylate) column and the resolved enantiomers were racemized upon UV irradiation.[39,40]

Other examples in which the central carbon was linked to two oxygen in 2,2'-spirochromene derivatives **7** and 2-oxaindan spiropyrane derivatives **8** were reported by Mannschreck and colleagues.[41–43] Spirochromene **7** was selected to illustrate the concept of enantiomeric enrichment of stereolabile chiral compounds by dynamic (D)HPLC.[44] Spiro(cyclohexadiene-indolines) provided examples in which the central carbon was linked to three carbon atoms and a nitrogen.[45] Cases in which the central carbon atom was linked to a nitrogen, an oxygen, and two carbon atoms such as in **9** were reported.[46–48] In all the previous cases, the enantiomers of **7**, **8**, and **9** were obtained by liquid chromatography on chiral support. To the best of our knowledge, a single article reported spiro compounds **10** in which the central carbon atom was linked to a sulfur and two nitrogens. In **10**, the barriers were determined by DNMR.[49] In contrast to compound **4**, the ground state is dipolar in **10**, while the open form is neutral. Spiro compound **11** provided an example in which

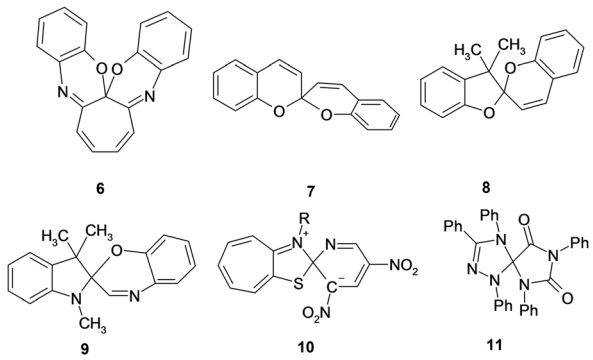

Scheme 4. Structures of selected examples of spiro compounds which have been resolved into enantiomers and thermally or photochemically racemized in the literature (except compound **11**)

the central carbon was attached to three nitrogen atoms and a carbonyl group.[50,51] However, in contrast to the selected examples **7–10**, the chirality issues and racemization were not addressed in **11**.

CONCLUSION

Spiro compound **4** was solely described during a 14-year period between 1964 and 1978. According to Scifinder, it is available for screening in three commercial libraries and from the excellent synthesis of that compound which was disclosed in 1968 from quaternized 2-chlorobenzothiazole and 2-(methylamino)benzenethiol.[7] The availability of spiro compound **4** in large amounts justifies our efforts to study that compound which was in our case a minor by-product during the synthesis of **1**. Our study shows that compound **4** and probably other *N*-substituted analogs can be viewed as a masked thiophenate attached to a benzothiazolium framework. Several applications of that unique property can be envisioned in material or labeling experiments after a fine tuning of the substitution pattern. This work is in progress.

ACKNOWLEDGMENTS

Dedicated to Professor Jacques Metzger (1921-2014). The Erasmus program is thanked for a grant (to V.R.). Aix-Marseille University, CNRS, and Chirbase project are thanked for funding. Paulina Jimenez Meneses is thanked for skillful assistance.

SUPPORTING INFORMATION

Additional supporting information may be found in the online version of this article at the publisher's web-site.

LITERATURE CITED

1. Koizumi T, Bashir N, Kennedy AR, Murphy JA. Diazadithiafulvalenes as electron donor reagents. J Chem Soc Perkin Trans 1999; 1: 3637–3643.
2. Budagumpi S, Haque RA, Salman AW. Stereochemical and structural characteristics of single- and double-site Pd(II)-N-heterocyclic carbene complexes: Promising catalysts in organic syntheses ranging from C-C coupling to olefin polymerizations. Coord Chem Rev 2012; 256: 1787–1830.
3. Yen SK, Koh LL, Hahn FE, Huynh HV. Hor TSA. Convenient entry to mono- and dinuclear palladium(II) benzothiazolin-2-ylidene complexes and their activities toward Heck coupling. Organometallics 2006; 25: 5105–5112.
4. Metzger J, Larivé H, Dennilauler R, Baralle R, Gaurat C. Comportement et réactivité d'hétérocycloammoniums dans la synthèse de colorants cyanines et carbocyanines. I . Dérivés du benzothiazolium. Bull Soc Chim Fr 1964; 2857–2867.
5. Vorsanger JJ. Etudes dans la série benzothiazolique-action des bases sur le methylsulfate de methyl-3-benzothiazolium. Bull Soc Chim Fr 1964; 119–122.
6. Wanzlick HW, Kleiner HJ, Lasch I, Füldner HU, Steinmaus H. Nucleophilic carbene chemistry. XII. Benzo- and naphtho[2,1-d]thiazolium salts. Liebigs Ann Chem 1967; 708: 155–169.
7. Quast H, Schmitt E. Preparation of heterocyclic spirans. Chem Ber 1968; 101: 1137–1139.
8. Takamizawa A, Hirai K, Hamashima Y, Sato H. Pyrimidine derivatives and related compounds. LXIV. Reaction of benzazolium salts with base. Chem Pharm Bull 1969; 17: 1462–1466.
9. Hocker J, Merten R. Parabanic acid derivatives. Chemistry of nucleophilic carbenes. Liebigs Ann Chem 1971; 751: 145–154.
10. Akiba KY, Kawamura T, Ochiumi M, Inamoto N. Chemistry of nitrosoimines. XV. Reactions of 3-substituted 2-nitrosoimino-2,3-dihydrobenzothiazoles with lithium aluminum hydride and diazo compounds. Bull Chem Soc Jpn 1976; 49: 1913–1916.
11. Gleiter R, Haider R, Quast H. Photoelectron spectroscopic investigation of heterocyclic spirans. J Chem Res (Synopsis) 1978; 138–139.
12. Diaper CM. Other tetrahetero-substituted methanes. Sci Synth 2005; 18: 1203–1282.
13. Yang Y, Zhang X, Zeng W, Huang H, Liang Y. Copper catalyzed three-component synthesis of benzothiazoles from o-iodoanilines, DMF, and potassium sulfide. RSC Adv 2014; 4: 6090–6093.
14. Furche F, Rappoport D. Theoretical and computational chemistry. In: Olivucci M editor, Density functional methods for excited states: equilibrium structure and electronic spectra. Elsevier: Amsterdam; 2005.
15. Bauernschmitt R, Ahlrichs R. Treatment of electronic excitations within the adiabatic approximation of time dependent density functional theory. Chem Phys Lett 1996; 256: 454–464.
16. Yanai T, Tew D, Handy N. A new hybrid exchange–correlation functional using the Coulomb-attenuating method (CAM-B3LYP). Chem Phys Lett 2004; 393: 51–57.
17. Frisch MJ, Trucks GW, Schlegel HB, et al. Gaussian 09, Revision D.01. Gaussian Inc.: Wallingford, CT; 2013.
18. Spackman MA, Jayatilaka D. Hirshfeld surface analysis. Cryst Eng Comm 2009; 11: 19–32.
19. Spackman MA, McKinnon JJ. Fingerprinting intermolecular interactions in molecular crystals. Cryst Eng Comm 2002; 4: 378–392.
20. Wolf C. Dynamic stereochemistry of chiral compounds, principles and applications. RSC Publishing: Cambridge, UK; 2008. p 159–164.
21. D'Acquarica I, Gasparrini F, Pierini M, Villani C, Zappia G. Dynamic HPLC on chiral stationary phases: a powerful tool for the investigation of stereomutation processes. J Sep Sci 2006; 29: 1508–1516.
22. Vanthuyne N, Roussel C. Chiroptical detectors for the study of unusual phenomena in chiral chromatography in differentiation of enantiomers. Schurig V (editor). Top Curr Chem 2013; 340: 107–151.
23. For other examples of plateau shape chromatograms see:Ciogli A, Dalla Cort A, Gasparrini F, Lunazzi L, Mandolini L, Mazzanti A, Pasquini C, Pierini M, Schiaffino L, Mihan FY. Enantiomerization of chiral uranyl-salophen complexes via unprecedented ligand hemilability: Toward configurationally stable derivatives. J Org Chem 2008; 73: 6108–6118.
24. Roussel C, Vanthuyne N, Bouchekara M, Djafri A, Elguero J, Alkorta I. Atropisomerism in the 2-arylimino-N-(2-hydroxyphenyl)thiazoline series: Influence of hydrogen bonding on the racemization process. J Org Chem 2008;73:403–411.
25. Piron F, Vanthuyne N, Joulin B, Naubron JV, Cismas C, Terec A, Varga RA, Roussel C, Roncali J, Grosu I. Synthesis, structural analysis, and chiral Investigations of some atropisomers with EE tetrahalogeno-1,3-butadiene core. J Org Chem 2009; 74: 9062–9070.
26. Ciogli A, Bicker W, Lindner W. Determination of enantiomerization barriers of hypericin and pseudohypericin by dynamic high-performance liquid chromatography on immobilized polysaccharide-type chiral stationary phases and off-column racemization experiments. Chirality 2010; 22: 463–471.
27. Hinterwirth H, Laemmerhofer M, Preinerstorfer B, Gargano A, Reischl R, Bicker W, Trapp O, Brecker L, Lindner W. Selectivity issues in targeted metabolomics: Separation of phosphorylated carbohydrate isomers by mixed-mode hydrophilic interaction/weak anion exchange chromatography. J Sep Sci 2010; 33: 3273–3282.
28. Cannazza G, Carrozzo MM, Battisti U, Braghiroli D, Parenti C, Troisi A, Troisi L. Determination of kinetic parameters of enantiomerization of benzothiadiazines by DCXplorer. Chirality 2010; 22: 789–797.
29. Carrozzo MM, Cannazza G, Battisti U, Braghiroli D, Troisi L, Parenti C. Epimerization and hydrolysis of 3,6-dimethyl-2,3,5,6-tetrahydro [1,2,4]thiadiazino[6,5,4-hi]indole 1,1-dioxide. J Chromatogr A2010;1217: 8136–8145.
30. Paul B, Butterfoss GL, Boswell MG, Renfrew PD, Yeung FG, Shah NH, Wolf C, Bonneau R, Kirshenbaum K. Peptoid atropisomers. J Am Chem Soc 2011; 133: 10910–10919.
31. Paul B, Butterfoss GL, Boswell MG, Huang ML, Bonneau R, Wolf C, Kirshenbaum K. N-Naphthyl peptoid foldamers exhibiting atropiso merism. Org Lett 2012; 14: 926–929.
32. Rizzo S, Benincori T, Bonometti V, Cirilli R, Mussini PR, Pierini M, Pilati T, Sannicolo F. Steric and electronic effects on the configurational stability of residual chiral phosphorus-centered three-bladed propellers: tris-aryl phosphanes. Chem Eur J 2013; 19: 182–194.
33. Maier F, Trapp O. The stereodynamics of 5,5'-disubstituted BIPHEPs. Chirality 2013; 25: 126–132.

34. Bentley KW, Wolf C. Comprehensive chirality sensing: development of stereodynamic probes with a dual (chir)optical response. J Org Chem 2014; 79: 6517–6531.
35. Diaz JE, Vanthuyne N, Rispaud H, Roussel C, Vega D, Orelli LR. Atropisomerism in amidinoquinoxaline N-oxides: effect of the ring size and substituents on the enantiomerization barriers. J Org Chem 2015; 80: 1689–1695.
36. Trapp O, Schurig V. Novel direct access to enantiomerization barriers from peak profiles in enantioselective dynamic chromatography: Enantiomerization of dialkyl-1,3-allenedicarboxylates. Chirality 2002; 14: 465–470.
37. Trapp O, Trapp G, Schurig V. Direct calculation and computer simulation of the enantiomerization barrier of oxazepam in dynamic HPLC experiments — a comparative study. J Biochem Biophys Methods 2002; 54: 301–313.
38. Ceccacci F, Mancini G, Mencarelli P, Villani C. Determination of the rotational barrier of a chiral biphenyl: comparisonof theoretical and experimental data. Tetrahedron: Asymmetry 2003; 14: 3117–3122.
39. Okamoto Y, Honda S, Yuki H, Nakamura N, Iitaka Y, Nozoe T. Resolution, absolute-configuration, and photoracemization of chiral troponoid acetals, cyclohepta[2,1-B-2,3-B']di[1,4]benzoxazines. Chem Lett 1984; 1149–1152: .
40. Harada N, Uda H, Nozoe T, Okamoto Y, Wakabayashi H, Ishikawa S. Absolute stereostructure of novel chiral troponoid spiro compounds as determined by theoretical calculation of CD spectra. J Am Chem Soc 1987; 109: 1661–1665.
41. Stephan B, Zinner H, Kastner F, Mannschreck A. Chiral 2H-pyrans. 2. Enantiomers of 2,2'-spirobichromenes — energy barrier for thermal racemisation during HPLC on tribenzoylcellulose. Chimia 1990; 44: 336–338.
42. Stephan B, Mannschreck A, Voloshin NA, Volbushko NV, Minkin VI. Separation and photoinduced transformations of the enantiomers of 3,3'-dimethylspiro[2H-1-benzopyran-2,1'(2)oxaindans. Tetrahedron Lett 1990; 31: 6335–6338.
43. Loncar-Tomaskovic L, Lorenz K, Hergold-Brundic A, Mrvos-Sermek D, Nagl A, Mintas M, Mannschreck A. Spirobinaphthopyrans: synthesis, x-ray crystal structure, separation of enantiomers, and barriers to thermal racemization .Chirality 1999;11:363–372.
44. Lorenz K, Yashima E, Okamoto Y. Enantiomeric enrichment of stereolabile chiral spiro compounds by dynamic HPLC on chiral stationary phases. Angew Chem Int Ed 1998; 37: 1922–1925.
45. Zimmermann T, Pustet N, Mannschreck A. The enantiomers of spiro (cyclohexadiene-indolines) and their thermal racemization. Monatsh Chem 1999; 130: 355–361.
46. Leiminer A, Stephan B, Mannschreck A. The enantiomers of indolino spiro compounds – barriers to thermal cleavage of their C(SP(3))-O bond. Mol Cryst Liq Cryst 1994; 246: 215–221.
47. Loncar-Tomaskovic L, Pustet N, Mrvos-Sermek D, Nagl A, Mintas M, Mannschreck A. Spirobipyridopyrans and indolinospiropyridopyrans: Synthesis, X-ray crystal structure, separation of enantiomers, and barriers to thermal cleavage of the C(sp(3))-O bond. Chirality 2001; 13: 81–88.
48. Bautista-Barrufet A, Lopez-Gallego F, Rojas-Cervellera V, Rovira C, Pericas MA, Guisan JM, Gorostiza P. Optical control of enzyme enantioselectivity in solid phase. ACS Catal 2014; 4: 1004–1009.
49. Olekhnovich LP, Budarina ZN, Lesin AV, Kurbatov SV, Borodkin GS, Minkin VI. Intramolecular inversion of configuration at tetrahedral carbon centers in dipolar spiro-delta-complexes of aminothiotropones – a dynamic NMR spectral study. Mendeleev Commun 1994; 4: 162–164.
50. Enders D, Breuer K, Runsik J, Teles JH. Chemical reactions of the stable carbene 1,3,4-triphenyl-4,5-dihydro-1H-1,2,4-triazol-5-ylidene. Liebigs Ann 1996; 2019–2028.
51. Matsuoka S-I, Tochigi Y, Takagi K, Suzuki M. Sequential one-pot and three-component reactions of an N-heterocyclic carbene to form 4-(1,2,4-triazol-5-ylidene)pyrrolidine-2,5-diones: a tandem umpolung/annulation sequence via deoxy-Breslow intermediates. Tetrahedron 2012; 68: 9836–9841.